Formation Pathways from 2,4,5-Trichlorophenol (TCP) to Polychlorinated Dibenzo-*p*-dioxins (PCDDs): An ab Initio Study

Yasuharu Okamoto* and Mutsumi Tomonari

Fundamental Research Laboratories, NEC Corporation, Tsukuba, Ibaraki 305-8501, Japan

Received: April 27, 1999

The formation mechanism of polychlorinated dibenzo-*p*-dioxins (PCDDs) has been studied for the first time by ab initio calculations. We examined twelve possible formation pathways from 2,4,5-TCP to three PCDD isomers (2,3,7,8-TCDD, 1,2,4,7,8-PeCDD, and 1,2,4,6,7,9-HxCDD). Four pathways by direct intermolecular condensation of two 2,4,5-TCP molecules and eight pathways via radicals were considered. We found that 2,3,7,8-TCDD is the only one of the three PCDD isomers produced when the reactions proceed by direct condensation from 2,4,5-TCP. However, when the reactions proceed through radicals, two path types seem to compete with each other. At low temperatures, one path type prefers to form TCDD, and the other prefers to form PeCDD.

1. Introduction

Polychlorinated dibenzo-*p*-dioxins (PCDDs) are notorious for their acute and chronic toxicity and their carcinogenic, teratogenic, and mutagenic effects. Recently, PCDDs are also suspected to be environmental endocrine disruptors that disturb the balance of hormones and damage the metabolism, immunity, and reproduction of exposed organisms.[1] In many countries (e.g., Netherlands,[2] Switzerland,[3] Japan and Canada[4]), PCDDs are produced in municipal waste incinerators and industrial heating facilities during the combustion of chlorine-containing plastics, and the formation of PCDDs seems to be ubiquitous to all combustion processes of such materials.

Several mechanisms leading to the formation of PCDDs during combustion have been proposed.[5,6] The formation of PCDDs in municipal waste incinerators is very complicated, because it involves a variety of chemical compounds and reactions. Moreover, some reactions are thought to be catalyzed by flyash.[7] Although an understanding of the elementary processes that govern the formation of PCDDs during combustion is needed to elucidate and control their formation, experiments on these elementary processes have been hindered by the strong toxicity of PCDDs. In such a situation, ab initio calculations can be an alternative. Moreover, the fundamental approach of ab initio calculation might shed new light on the study of dioxins. There have been a few ab initio calculations made,[8−10] but these were aimed mainly at clarifying the possibility of a nonplanar structure and butterfly motion of the dioxin ring.[8,9]

In this report, we discuss the first ab initio study on the formation of PCDDs. We examined twelve formation pathways from 2,4,5-trichlorinated phenol (TCP) to three possible isomers of PCDDs: 2,3,7,8-tetrachlorinated dibenzo-*p*-dioxin (TCDD), 1,2,4,7,8-pentachlorinated dibenzo-*p*-dioxin (PeCDD), and 1,2,4,6,7,9-hexachlorinated dibenzo-*p*-dioxin (HxCDD). We focused especially on 2,3,7,8-TCDD (Figure 1), because its toxicity is the strongest among all 75 PCDD isomers.[11] To form the dioxin ring, the substituent at the ortho site of the hydroxy group (−OH) of polychlorinated phenols (PCPs) serves as an elimination group. Among the PCPs, 2,4,5-TCP, which has a Cl atom substituted at its ortho site, has the minimum number of Cl atoms to form 2,3,7,8-TCDD. PCPs such as 2,4,5-TCP are considered possible precursors[12,13] for PCDDs in the de novo formation[14] from chlorine-containing plastics in incinerators. In the combustion process, we expected the pathways through the 2,4,5-TCP radical (hereafter we refer to this radical as 2,4,5-TCPR) to be involved in the formation of PCDDs from 2,4,5-TCP. In addition to pathways via the radical, the direct intermolecular condensation of two 2,4,5-TCP molecules at high temperatures should be considered. We considered both cases and estimated the product ratio of the above three PCDD isomers in each case by analyzing the activation energies and by applying transition-state theory combined with ab initio calculations. We found that 2,3,7,8-TCDD is the only one of these three PCDD isomers produced when the reactions proceed by direct condensation from 2,4,5-TCP. On the other hand, when the reaction proceeds through radicals from 2,4,5-TCP, two pathways (which are distinguished by the sequence of the radical reactions) seem to compete with each other.

Figure 1. Optimized geometries of 2,3,7,8-TCDD at the B3LYP/6-31G(d′,p′) level of theory. In this and Figure 4, the yellow, purple, red, and blue balls, respectively, stand for carbon, hydrogen, oxygen, and chlorine atoms.

2. Computational Scheme

We used the hybrid-density functional scheme (B3LYP) proposed by Becke who successfully combined the Hartree−Fock exchange potential with the exchange-correlation potential

10.1021/jp991383u CCC: $18.00
Published on Web 09/03/1999

TABLE 1: Calculated Molecular Geometries (in Angstroms or Degrees) and Vibrational Frequencies (in cm^{-1}) of 2,3,7,8-TCDD at the B3LYP/6-31G(d′,p′) Level of Theory

bond length	C_A-O_1[a] = 1.378 (1.379)[b]	C_A-C_1 = 1.388 (1.377)	C_1-C_2 = 1.398 (1.384)	C_2-C_3 = 1.400 (1.385)
	C_A-C_B = 1.400 (1.387)	C_1-H_1 = 1.084 (1.01)	C_2-Cl_2 = 1.745 (1.728)	
bond angle	$\angle C_AO_1C_D$ = 115.9 (115.7)	$\angle O_1C_AC_1$ = 118.0 (117.6)	$\angle C_AC_1C_2$ = 120.2 (121)	$\angle C_1C_2Cl_2$ = 118.5 (118.9)
	$\angle C_AC_1H_1$ = 119.2 (119)	$\angle O_1C_AC_B$ = 122.0 (122.2)		
vibrational frequency[c]	COC(sym stretching)	897 (895)	885 (916)	935 (932)
	ring breathing	1129 (1103)		
	CCC (ring bending)	1187 (1173)		
	CH (in-plane deformation)	1237 (1248)		
	COC (asym stretching)	1325 (1306)	1343 (1321)	
	skeletal vibrations	1515 (1465)	1615 (1566)	

[a] See Figure 1 for the carbon-atom subscript. [b] The values in parentheses were determined by experiment and were obtained from ref 16 for the geometrical parameters and ref 17 for the vibrational frequencies. [c] The scale factor was not used for evaluation of the vibrational frequencies. See ref 9 for the specifications of the vectors of vibration.

based on the density functional theory (DFT).[15] The 6-31G(d′,p′) basis set was used to obtain stable molecular structures, transition states, vibrational frequencies, and the intrinsic reaction coordinates. To improve the accuracy of the calculated energies, the single-point B3LYP energy calculations were done with the much larger 6-311++G(2d,2p) basis set at the geometries obtained by using the 6-31G(d′,p′) set. Zero-point vibrational energies (ZPVEs) were also included in our evaluation of the reaction and activation energies. Following the conventional notation in quantum chemistry, this procedure is denoted as B3LYP/6-311++G(2d,2p)//B3LYP/6-31G(d′,p′) + ZPVE(B3LYP/6-31G(d′,p′)). All the calculations in this report were done using the Gaussian 94 program[16] installed on the NEC SX4 supercomputing system.

To check the validity of our computational scheme, we calculated the stable molecular geometry and vibrational frequencies of 2,3,7,8-TCDD (Figure 1) and compared them with experimental values.[17,18] As shown in Table 1, the computed geometrical parameters differed from the experimental ones by −0.7% to +1.1% (except for the C−H bond), and the computed frequencies differed from the experimental ones by −3.4% to +3.5%. This confirmed the reliability of our computational method for both the molecular geometry and vibrational frequency.

3. Results and Discussion

Twelve Formation Pathways to PCDDs. We will begin our examination of the PCDD formation process by explaining the reaction scheme considered in this report. Pathways to the three PCDD isomers are schematically shown in Figure 2. The pathways to polychlorinated 2-phenoxyphenols (predioxin A and B in Figure 2) were classified into three path types α, β, and γ. Path types α (solid arrows) and β (dotted arrows) both pass through the 2,4,5-TCPR. On the other hand, path type γ (bold white arrows) represents direct intermolecular condensation that is not via the 2,4,5-TCPR. In path types α and β, a H radical and 2,4,5-TCPR are formed by the O− H bond of 2,4,5-TCP breaking. In path type α, the H radical reacts with another 2,4,5-TCP and forms new radicals (R_A or R_B in Figure 2). Then, R_A and R_B react with 2,4,5-TCPR and form predioxins A and B, respectively. On the other hand, in path type β, the 2,4,5-TCPR reacts with another 2,4,5-TCP and forms intermediates (M_A or M_B in Figure 2). These intermediates react with the H radical and form the predioxins A and B. To form a dioxin ring, reactions must occur at the ortho site of the hydroxy group of 2,4,5-TCP. Thus, there are two possible reaction sites, as denoted by the A or B subscripts in Figure 2, which lead to 6 (=3 × 2) formation pathways from 2,4,5-TCP to the predioxins. After the formation of the predioxins, intramolecular condensation (the bold black arrows in Figure 2) with the desorbing HCl or H_2 molecule leads to the above three PCDD isomers. Also there are two reaction sites in this reaction. Thus, in Figure 2, we have 12 (=6 × 2) pathways in total. In short, each pathway considered here is composed of three parts: (i) the reaction path through either 2,4,5-TCPR (α and β) or not (γ), and path types α and β distinguished by the sequence of the reaction of 2,4,5-TCP; (ii) the two ortho sites of 2,4,5-TCP (A and B); and (iii) two molecules (HCl and H_2) that desorb from predioxin A or B. Thus, pathways can be denoted, for example, as path-(α_A_HCl) as shown in Figure 3A.

The reaction energy and activation energy (if it exists) of each elementary process is given in Table 2. In the following, we consider some of the characteristic points of each elementary process that comprises these formation pathways.

Pathways to the Predioxins via Radicals. Breaking the O−H bond of 2,4,5-TCP forms a radical (2,4,5-TCPR) and a hydrogen radical. This is a highly endothermic reaction (Table 2). There is no TS in this reaction because the potential curve is attractive along the O−H distance. Then, as stated, the sequence of the radical reactions creates two path types. In the α path type, the H radical abstracts a Cl or H atom from the ortho site of the hydroxy group of another 2,4,5-TCP and forms radical R_A or R_B (Figure 2). The TSs of these abstraction reactions are shown in Figure 4A. Then, R_A or R_B reacts with 2,4,5-TCPR and forms predioxins A or B (Figure 4B) in highly exothermic reactions (Table 2). The Cl abstraction (R_A) is exothermic, whereas the H abstraction (R_B) is endothermic. Moreover, the activation energy of the former abstraction is 0.18 eV smaller than that of the latter. Thus, the formation of predioxin A is more favorable than that of predioxin B. On the other hand, in the β path type, 2,4,5-TCPR attacks the carbon atoms of a 2,4,5-TCP at the ortho sites of its hydroxy group and the intermediates M_A (Cl-side carbon attacked: Figure 4B) and M_B (H-side carbon attacked: Figure 4B) are formed. Both of these reactions are endothermic and reaction energies are about 0.76 eV. From Table 2, we find the activation energy of M_B is about 0.06 eV lower than that of M_A, which indicates the formation of M_B is more favorable than that of M_A. Intermediates M_A and M_B have one sp^3 carbon in their benzene ring (Figure 4B). Thus, they react with H radicals and form more stable intermediates (predioxin A or B in Figure 4B) while giving off a large amount of energy (Table 2).

Pathways to the Predioxins by Intermolecular Condensation. Path type γ corresponds to the intermolecular condensation of two 2,4,5-TCP molecules desorbing a HCl or a H_2 molecule. The TSs of these intermolecular reactions are shown in Figure 4C. This path type also leads to the predioxins A and B (Figure 4B). In this case, the reaction barrier of HCl desorption is about

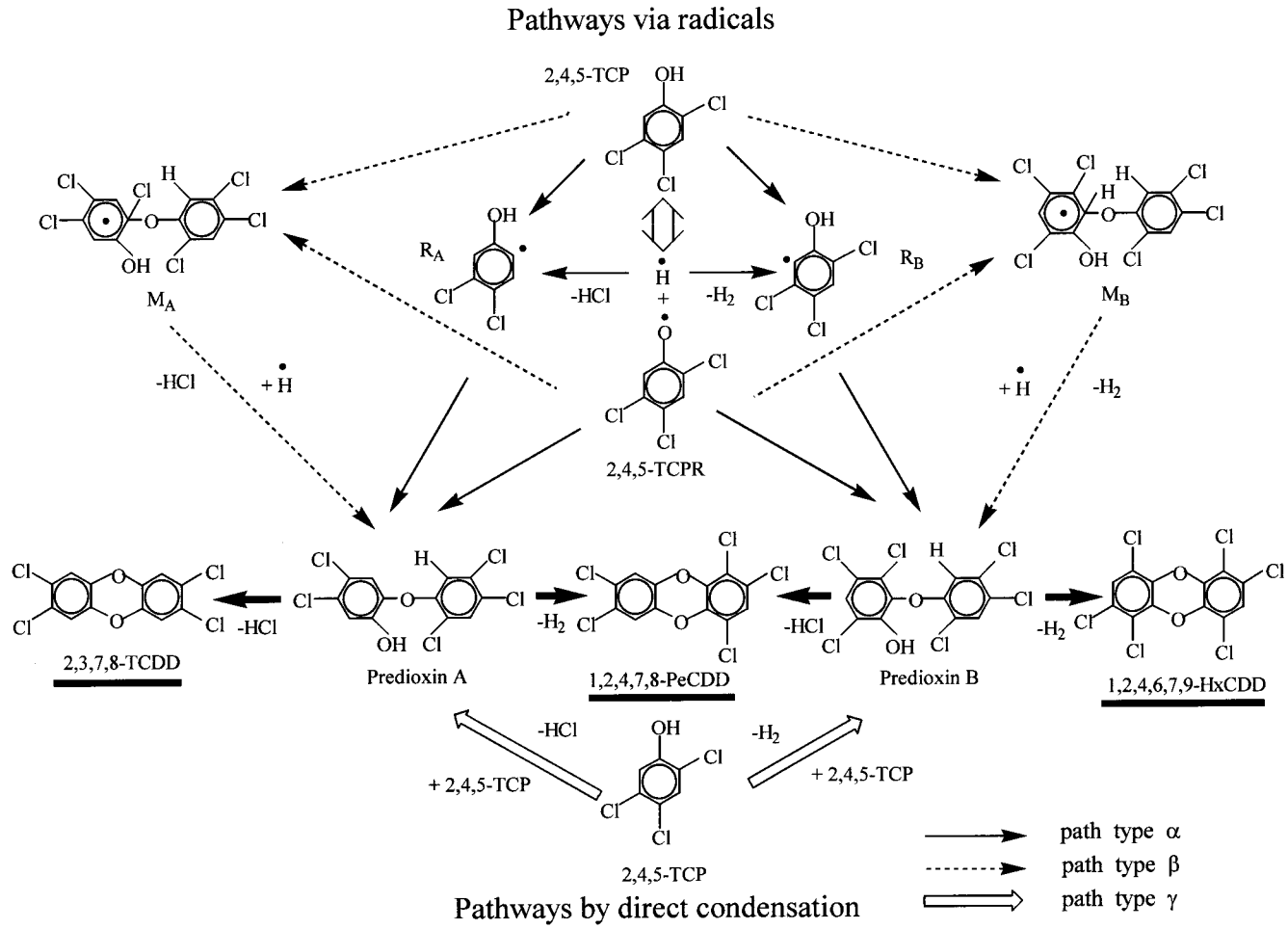

Figure 2. Twelve pathways form 2,4,5-TCP to three PCDD isomers. Solid arrows correspond to path type α and dotted arrows correspond to path type β. Both path types pass via 2,4,5-TCPR. Bold white arrows correspond to path type γ, which is the direct condensation of two 2,4,5-TCP molecules. Bold black arrows correspond to the intramolecular condensation of predioxins.

2 eV lower than that of H_2 desorption. Moreover, the reaction energy of HCl desorption is almost zero, whereas H_2 desorption is endothermic by about 1 eV. Therefore, the formation of predioxin A is much more favorable than that of predioxin B. As will be explained below, the fact that HCl desorption is much more favorable than H_2 desorption is also true of the intramolecular condensation of the predioxins to PCDDs.

Intramolecular Condensation: Formation of the Dioxin Ring. The HCl desorption by intramolecular condensation of the predioxin A gives 2,3,7,8-TCDD, and H_2 desorption from predioxin A leads to 1,2,4,7,8-PeCDD (Figure 2). We found that the noncoplanar predioxin A (Figure 4B) is about 1.3 eV more stable than coplanar predioxin A. The coplanar predioxin is metastable, having two imaginary frequencies. Similarly, HCl desorption by intramolecular condensation of the predioxin B gives 1,2,4,7,8-PeCDD, and H_2 desorption from predioxin B gives 1,2,4,6,7,9-HxCDD (Figure 2). From Table 2, we found the reaction and activation energies of these forms of intramolecular condensation are similar to those of the above intermolecular condensation: the reaction energy of HCl desorption is almost zero and its activation energy is about 2.3 eV, whereas the reaction energy of H_2 desorption is about 1 eV and its activation energy is about 4.5 eV. Thus, as mentioned, desorption of HCl is more favorable than that of H_2 in intramolecular condensation, as was shown for the intermolecular condensation. The TSs of these intramolecular reactions are shown in Figure 4D.

The TS of the intramolecular reaction of predioxin A to the product (2,3,7,8-TCDD + HCl) is shown in Figure 4D (upper left), and the intrinsic reaction coordinates (IRCs) around the four-center $TS_{HCl\ A}$ are shown in Figure 5. An IRC is defined as the minimum energy path connecting the reactant to the product via the TS. The IRC calculation follows the path both forward and backward from the TS while optimizing the geometry of the system at each point along the path. In Figure 5, $s = 0$ corresponds to the TS of this reaction and, in the $s > 0$ ($s < 0$) region, the system is approaching the product (reactant). We calculated 40 points for the forward ($s > 0$) direction and 80 points for the backward ($s < 0$) direction with a step size of 0.07 amu$^{-1/2}$ bohr. In Figure 5, R(O−H) and R(C−Cl) increase in length, respectively, from 0.96 to 1.58 Å and from 1.79 to 2.58 Å. In contrast, the lengths of R(C−O) and R(H−Cl) decrease from 2.42 to 1.52 Å and 2.32 to 1.30 Å, respectively. This clearly shows that both O−H and C−Cl bonds break during the reaction, while both C−O and H−Cl bonds form. We found that the dioxin ring is bent at the TS (Figure 4D). As pointed out by Schaefer and Sebastian[8] and Fujii et al.[9] the energy loss caused by the bending of the dioxin ring is small. Thus, steric hindrance is reduced in the TS of HCl desorption due to bending of the dioxin ring.

Energy Profile and the Product Ratio of the Three PCDD Isomers. Having examined the elementary reaction processes, we are now in a position to discuss the favorable formation pathways. The energy profiles that correspond to the 12

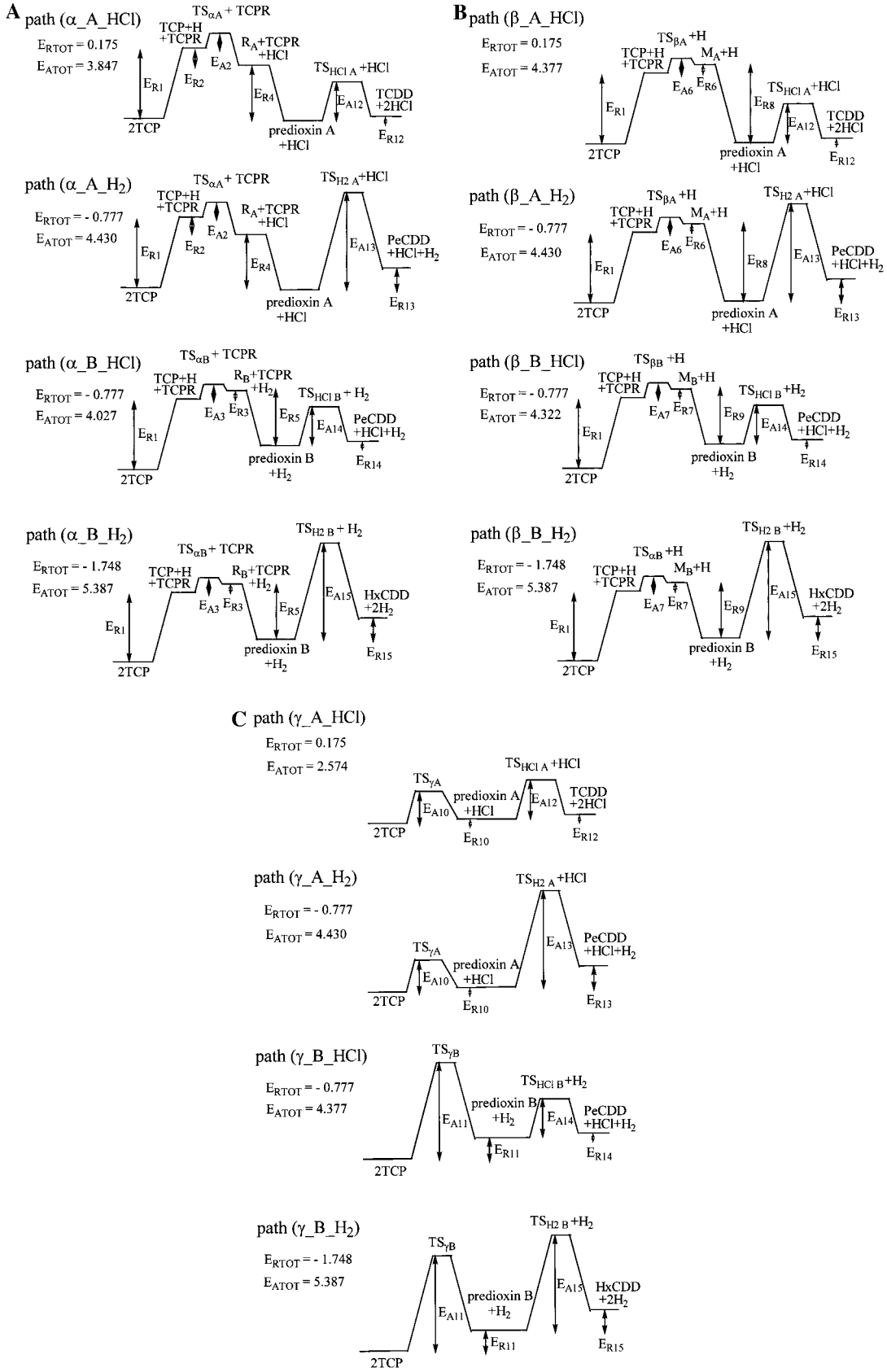

Figure 3. Energy profiles of the PCDD formations from 2,4,5-TCP, α path type (A), *β* path type (B), and *γ* path type (C). E_{RTOT} and E_{ATOT}, respectively, stand for overall reaction and activation energies of the pathway. See Table 2 for the values E_{Rn} and E_{An}. In the reaction energies, minus means the reaction is endothermic.

pathways considered here are shown in Figure 3. We began by comparing the four pathways included in path type *γ*, which do not pass radicals (Figure 3C). As stated, in both intermolecular and intramolecular condensation, the activation energies of H_2 desorption are about 2 eV higher than those of HCl desorption, which suggests only HCl desorption occurs at low

TABLE 2: Reaction (E_R) and Activation Energies (E_A) (in eV) of the Elementary Processes Calculated at the B3LYP/6-311++G(2d,2p)//B3LYP/6-31G(d′,p′) + ZPVE(B3LYP/6-31G(d′,p′)) Level of Theory

	reaction energy[a]	activation energy
pathway via radical		
2,4,5-TCP → 2,4,5-TCPR	$E_{R1} = -3.488$	no[b]
(path type α)		
2,4,5-TCP + H → R_A + HCl	$E_{R2} = 0.479$	$E_{A2} = 0.359$
2,4,5-TCP + H → R_B + H_2	$E_{R3} = -0.317$	$E_{A3} = 0.539$
R_A + 2,4,5-TCPR → predioxin A	$E_{R4} = 3.065$	no
R_B + 2,4,5-TCPR → predioxin B	$E_{R5} = 2.854$	no
(path type β)		
2,4,5-TCP + 2,4,5-TCPR → M_A	$E_{R6} = -0.760$	$E_{A6} = 0.889$
2,4,5-TCP + 2,4,5-TCPR → M_B	$E_{R7} = -0.758$	$E_{A7} = 0.834$
M_A + H → predioxin A + HCl	$E_{R8} = 4.304$	no
M_B + H → predioxin B + H_2	$E_{R9} = 3.294$	no
pathway by direct condensation (path type γ)		
2 × 2,4,5-TCP → predioxin A + HCl	$E_{R10} = 0.056$	$E_{A10} = 2.295$
2 × 2,4,5-TCP → predioxin B + H_2	$E_{R11} = -0.953$	$E_{A11} = 4.377$
intramolecular condensation		
predioxin A → 2,3,7,8-TCDD + HCl	$E_{R12} = 0.120$	$E_{A12} = 2.574$
predioxin A → 1,2,4,7,8-PeCDD + H_2	$E_{R13} = -0.832$	$E_{A13} = 4.486$
predioxin B → 1,2,4,7,8-PeCDD + HCl	$E_{R14} = 0.176$	$E_{A14} = 2.528$
predioxin B → 1,2,4,6,7,9-HxCDD + H_2	$E_{R15} = -0.795$	$E_{A15} = 4.436$

[a] In the reaction energies, minus means the reaction is endothermic. [b] no means that the transition state is not found in the elementary process.

temperature. Thus, we expected 2,3,7,8-TCDD to be the only product via the γ path type. On the other hand, in path types α and β (Figure 3A,B), the formation of 2,4,5-TCPR needs a large amount of energy (3.488 eV in Table 2). This suggests that path type γ is more favorable than path types α and β, unless the O−H bond of 2,4,5-TCP is broken by absorbing ultraviolet light or by some mechanism such as abstraction of a H atom in the hydroxy group by other radicals. However, after breaking of the O−H bond, the remaining substantial reaction barriers (from the state TCP + TCPR + H in Figure 3A and 3B) are much smaller than those of path type γ (Table 2 and Figure 3C). Moreover, in the final reactions of intramolecular condensation through path types α and β, HCl desorption is *barrierless* from the state TCP + TCPR + H, whereas H_2 desorption has a substantial reaction barrier. This suggests that HCl desorption is favored in the final reaction. Thus, we can safely assume that predioxin A forms 2,3,7,8-TCDD and predioxin B forms 1,2,4,7,8-PeCDD through path types α and β. Since the final intramolecular desorption of HCl is barrierless, the product ratio of 2,3,7,8-TCDD and 1,2,4,7,8-PeCDD is roughly given by the ratio of the radicals R_A and R_B in path type α and by the ratio of the intermediates M_A and M_B in path type β. This argument corresponds to the assumption that the product ratio is simply dependent on the rate-determining step of the whole reaction process (Figure 3). Using the transition-state theory (TST), we estimated the product ratio via radicals. The rate constant of the reaction (x) based on the TST is given by

$$k(x) = \frac{k_b T}{h} \exp\left(\frac{-\Delta G(x)}{k_b T}\right) \quad (1)$$

where T is temperature and k_b and h are Boltzmann's and Planck's constants, respectively. Gibbs's energy change is defined as $\Delta G = G(TS) - G(\text{reactant})$, Gibbs's energy ($G$) is defined by

$$G = H - TS \quad (2)$$

where H ($=E_0 + E_{ZPE} + E_{th} + \boldsymbol{RT}$) is enthalpy and S is entropy. E_0 is electronic energy, E_{ZPE} is zero-point energy, E_{th} is the sum of the thermal contribution from vibration, rotation, and translation, and RT is thermal enthalpy. All of these properties can be routinely calculated by a modern ab initio program. Since incompleteness of the basis set mainly influences the electronic energy (E_0), we used a value of E_0 that was evaluated with a large basis set (6-311++G(2d,2p)). The Gibbs energy changes of the rate-determining step at 300, 600, 900, and 1200 K for path type α (path(α_A_HCl) and path(α_B_HCl)) and path type β (path(β_A_HCl) and path(β_B_HCl)) are given in Table 3.

The ratio of the 2,3,7,8-TCDD to PCDDs (2,3,7,8-TCDD + 1,2,4,7,8-PeCDD) is obtained from the following equation and Table 3. (The formation of 1,2,4,6,7,9-HxCDD is expected to be negligible.)

$$\frac{[\text{TCDD}]}{[\text{PCDDs}]} \approx \frac{k(\text{A})}{k(\text{A}) + k(\text{B})} = \frac{\exp(-\Delta G(\text{A})/k_b T)}{\exp(-\Delta G(\text{A})/k_b T) + \exp(-\Delta G(\text{B})/k_b T)} \quad (3)$$

where A signifies R_A (path type α) and M_A (path type β) and B signifies R_B (path type α) and M_B (path type β). We found that the ratio of TCDD was 99.9%, 94.8%, 80.2%, and 63.3, respectively, at 300, 600, 900, and 1200 K via path type α, and was 9.6%, 24.1%, 32.0%, and 36.5%, respectively, via path type β.

4. Summary

We have performed ab initio calculations to examine the elementary processes and the formation pathways from 2,4,5-TCP to three PCDD isomers. Pathways by direct intermolecular condensation and those via radicals were considered. Unless the OH bond of 2,4,5-TCP is broken through the absorption of ultraviolet light or by some mechanism such as abstraction of a H atom in the hydroxy group by other radicals, pathways by direct condensation are favored compared to those via radicals. We found that 2,3,7,8-TCDD is the only one of the three PCDD isomers produced when the reactions proceed by direct condensation from 2,4,5-TCP. On the other hand, when the reactions proceed through radicals, two path types seem to compete with each other. In this situation at low temperatures, one path type prefers to form TCDD, but the other prefers to form PeCDD.

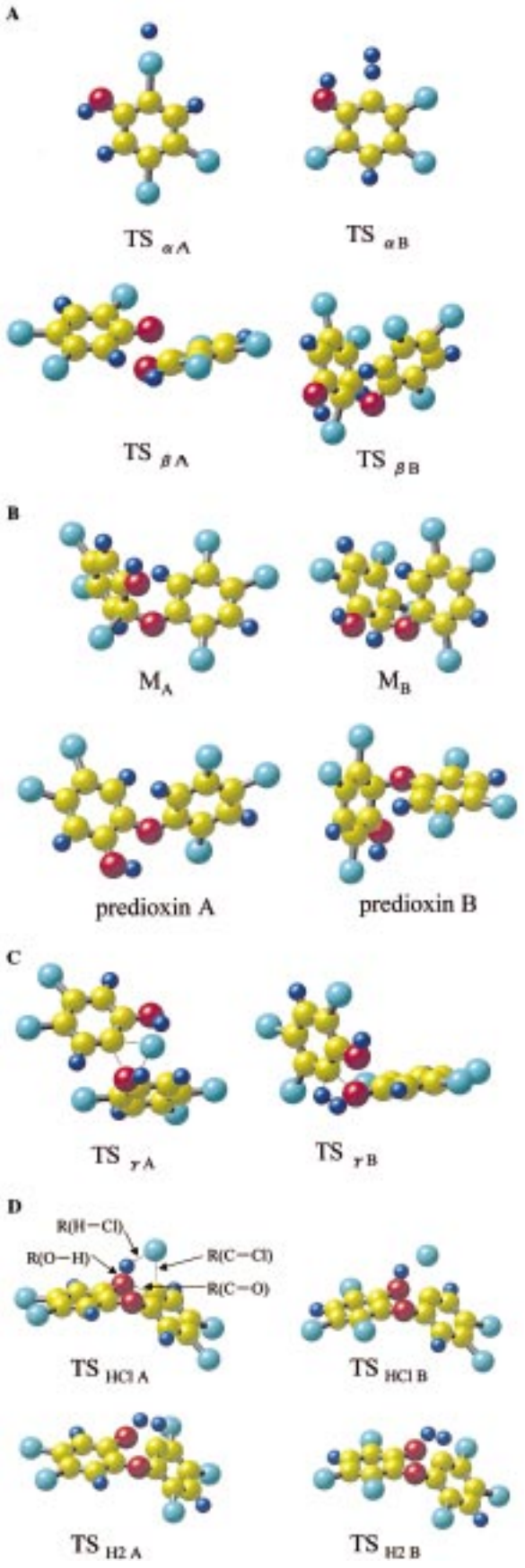

Figure 4. Optimized geometries of the first TSs (A) and intermediates in paths α and β (B), the first TSs in path γ (C), and TSs of the intramolecular condensation (D) obtained by the B3LYP/6-31G(d′,p′) level of theory.

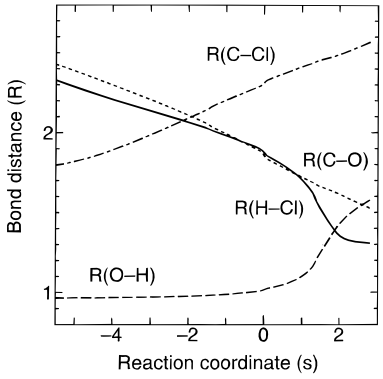

Figure 5. Intrinsic reaction coordinates (IRCs) of the reaction around the TS_{HCLA}. The unit of length of the reaction coordinates is $amu^{-1/2}$ bohr and that of the bond length is Å.

TABLE 3: Gibbs Energy Change ($\Delta G = G(TS) - G$(reactant), in eV) of the Rate-Determining Step of Path Type α (A, path(α_A_HCl); B, path(α_B_HCl)) and Path Type β (A, path(β_A_HCl); B, path(β_B_HCl))

temp (K)	ΔG(A)	ΔG(B)
	Path Type α	
300	0.606	0.782
600	0.910	1.060
900	1.233	1.342
1200	1.570	1.627
	Path Type β	
300	1.438	1.380
600	1.975	1.915
900	2.498	2.439
1200	3.012	2.955

References and Notes

(1) Spink, D. C.; Lincoln, D. W., II; Dickeman, H. W.; Gierthy, J. F. *Proc. Natl. Acad. Sci. U.S.A.* **1990**, *87*, 6917.

(2) Olie, K.; Vermeulen, P. L.; Hutzinger, O. *Chemosphere* **1997**, *6*, 455.

(3) Buser, H. R.; Bosshardt, H. P.; Rappe, C. *Chemosphere* **1978**, *7*, 165.

(4) Eiceman, G. A.; Clement, R. E.; Karasek, F. W. *Anal. Chem.* **1979**, *51*, 2343.

(5) Choudhry, G., et al. In *Chlorinated dioxins and related compounds impact on the environment*; Hutzinger, O., et al., Eds.; Pergamon Press: Oxford, U.K., 1982; p 275.

(6) Karasek, F. K. *Organohalogen Compounds* **1995**, *23*, 315.

(7) Vogg, H.; Stieglitz, L. *Chemosphere* **1986**, *15*, 1373.

(8) Schaefer, T.; Sebastian, R. *THEOCHEM* **1990**, *204*, 41.

(9) Fujii, T.; Tanaka, K.; Tokiwa, H.; Soma, Y. *J. Phys. Chem.* **1996**, *100*, 4810.

(10) Cheney, B. V.; Tolly, T. *Int. J. Quantum Chem.* **1979**, *16*, 87.

(11) Kimbrough, R. D. *Arch. Environ. Health* **1972**, *25*, 125.

(12) Karasek, F. K.; Dickson, L. C. *Science* **1987**, *237*, 754.

(13) Shaub, W. M.; Tsang, W. In *Human and Environmental Risks of Chlorinated Dioxins and Related Compounds*; Tucker, R. E., Young, A. L., Grey, A. P., Eds.; Plenum: New York, 1983; p 731.

(14) Stieglitz, L.; Zwick, G.; Beck, J.; Roth, W.; Vogg, H. *Chemosphere* **1989**, *18*, 1219.

(15) Becke, A. D. *J. Chem. Phys.* **1993**, *98*, 1372. Becke, A. D. *Phys. Rev. A* **1988**, *38*, 3098. Lee, C.; Yang, W.; Parr, R. G. *Phys. Rev. B* **1988**, *37*, 785.

(16) Frish, M. J.; Trucks, G. W.; Schlegel, H. B.; Gill, P. M. W.; Johnson, B. G.; Robb, M. A.; Cheeseman, J. R.; Keith, T. A.; Petersson, G. A.; Montgomery, J. A.; Raghavachari, K.; Al-Laham, M. A.; Zakrzewski, V. G.; Oritz, J. V.; Foresman, J. B.; Cioslowski, J.; Stefanov, B. B.; Nanayakkara, A.; Challacombe, M.; Peng, C. Y.; Ayala, P. Y.; Chen, W.; Wong, M. W.; Andres, J. L.; Replogle, E. S.; Gomperts, R.; Martin, R. L.; Fox, D. J.; Blinkley, J. S.; Defrees, D. J.; Baker, J.; Stewart, J. P.; Head-Gordon, M.; Gonzalez, C.; Pople, J. A. *Gaussian 94*; Gaussian, Inc.: Pittsburgh, PA, 1995.

(17) Boer, F. P.; Neuman, M. A.; Van Remoortere, F. P.; North, P. P.; Rinn, H. W. *Adv. Chem. Ser.* **1973**, *120*, 1.

(18) Grainger, J.; Reddy, V. V.; Patterson, D. G., Jr. *Chemosphere* **1989**, *18*, 981.